



RESPONSE OF A MULTI-LAYERED INFINITE CYLINDER TO TWO-DIMENSIONAL PRESSURE EXCITATION BY MEANS OF TRANSFER MATRICES

J. S. SASTRY

*Aeroelasticity and Structural Dynamics Group, Aeronautical Development Agency,
Bangalore-560 017, India*

AND

M. L. MUNJAL

*Centre of Excellence for Technical Acoustics, Department of Mechanical Engineering,
Indian Institute of Science, Bangalore-560 012, India*

(Received 20 July 1994, and in final form 12 August 1997)

A 6×6 transfer matrix is presented to evaluate the response of a multi-layered infinitely long elastic cylinder, imbedded in a fluid and enclosing another fluid, to a given two-dimensional pressure excitation on the outside or inside, or alternatively to evaluate the acoustic pressure distribution excited by the radial velocity components of the radiating surface. It is shown that the transfer matrix presented is a general case embodying the transfer matrix of one-dimensional pressure excitation due to a normal incident wave. It is also shown that the transfer matrix can be effectively used to obtain the scattering coefficient and noise reduction of a multi-layered cylinder for the case of oblique incidence of a plane wave. Numerical results for the scattering form function and noise reduction of a multi-layered infinite cylinder are given to illustrate the effect of two-dimensionality (angle of incidence), and layer material characteristics.

© 1998 Academic Press Limited

1. INTRODUCTION

The acoustical design of a shell that houses the transducer array in a cylindrical sonar system intended to operate in active and passive modes, and decipher the signal information of the echo/radiated wave that insonifies the dome wall, calls for studies related to the presence of various types of waves and associated resonances that set in during such excitation.

The studies concerning these phenomena for the case of oblique incidence have been made mainly by using the classical normal mode solutions [1–5], wherein the response of the cylindrical shell to a given pressure excitation and associated wave propagation is made by expressing the displacements and stresses in terms of the scalar and vector potential functions and formulating the characteristic equations in terms of their amplitudes by satisfying the interfacial and boundary conditions. In a recent paper, Leon *et al.* [6] used this approach to obtain the scattering form function for the case of oblique incidence on an infinitely long cylinder. For the case of a hollow cylinder analysis presented by them, the direct approach may seem to be appropriate. However, as the number of layers constituting the hollow cylinder wall increases, the algebra associated with the formulation of characteristic equations becomes cumbersome with the increase of six characteristic equations for each additional layer and increase in the resultant matrix size (the matrix

size being given by $(6n + 2) \times (6n + 2)$ where n is number of layers). It makes computation of the inverse or determinant of the coefficient matrix much slower and some times may even lead to numerical difficulties. On the other hand, the transfer matrix approach is best suited for the analysis of ducts and mufflers [7], multi-layer flat plates for one-dimensional as well as two-dimensional excitation [8, 9], and multi-layer cylinders for one-dimensional excitation [10]. In fact, the development of a transfer matrix was first presented by Thomson [11].

This paper is concerned with the derivation of a 6×6 transfer matrix connecting the state variables on either side of the multi-layered infinitely long cylinder to obtain the response of the shell, and scattering and transmission, in terms of elements of the overall transfer matrix for the case of oblique incidence. The model uses exact equations of elastodynamics, and construction of the solutions is done by using scalar and vector potentials. Solutions for the scalar and vector potentials in each layer are given in terms of Bessel functions. Following Brekhovskikh [12], interfacial conditions of continuity of pressure and velocities between the layers and appropriate radiation impedances on the exterior and interior of the multi-layered cylinder, have been used to obtain explicit expressions for the scattering coefficient and transmission coefficient in terms of elements of the transfer matrix. These expressions can be directly used for any number of layers by noting that the elements of the final matrix are obtained after multiplication of the elements of individual layers, with the resultant matrix remaining a 6×6 matrix irrespective of the number of layers.

Expressions have also been derived to evaluate the response of the multi-layered cylinder to a given two-dimensional pressure excitation on one of the faces (inside or outside) due to oblique incident waves which indeed would result in a three-dimensional stress field, unlike the case of one-dimensional pressure excitation due to normal incidence which would correspond to a two-dimensional distribution of stresses and velocities, upon taking into consideration the boundary conditions of zero shear and appropriate radiation loading on the exposed faces. Similar expressions would hold for the acoustic pressure excited by the radial velocity component of the exposed surface.

It is shown numerically that both the normal mode solution [6] and the present method yield exactly the same results. Also it is shown analytically that the transfer matrix reduces to a 4×4 transfer matrix presented in reference [10] for the limiting case of normal incidence and one-dimensional pressure excitation.

Numerical examples are given here for the case of a two-layered cylinder consisting of a visco-elastic layer backed by a metallic cylinder. Some parametric studies to illustrate the effect of two-dimensionality (angle of incidence), and the layer material characteristics have been carried out.

2. BASIC EQUATIONS

The geometry considered for the present problem is shown in Figure 1. The incident plane wave makes an angle ϕ_1 with the axis of symmetry of the multi-layered cylindrical shell, made up of m layers and having the inner and outer radii of each layer denoted by r_{in}^i and r_{out}^i , where i denotes the i th layer counted from the outside. The axis of the cylindrical shell is taken to be the z -axis of the cylindrical co-ordinate system (r, θ, z) . The cylinder is imbedded in a fluid having density ρ_0 and sound speed c_0 and encloses another fluid of density ρ_{m+1} having sound speed c_{m+1} . The transmitted wave makes an angle ϕ_2 with the innermost layer. The outermost layer 1 and the innermost layer m are in contact with the fluids. The six relevant state variables, the normal stress σ_{rr} , shear stresses $\tau_{r\theta}$ and τ_{rz} , and particle velocities V_r , V_θ and V_z in the radial, circumferential and axial directions,

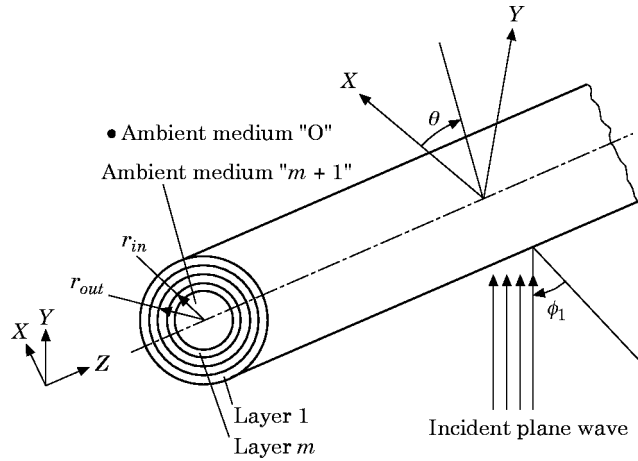


Figure 1. Multi-layered infinite cylinder with different wave components and their angles.

respectively, at the two faces of first layer are shown in Figure 2. r_{in} and r_{out} have also been shown for an intermediate layer.

Let the velocity vector field $\vec{V}(r, \theta, z)$ be separated into an irrotational part and a divergence-free part. In view of the identities $\text{curl grad } f \equiv 0$ and $\text{div curl } \vec{f} \equiv 0$, one can write [13]

$$\vec{V} = \text{grad } \phi + \text{curl } \vec{\phi}. \quad (1)$$

Thus,

$$V_r = \frac{\partial \phi}{\partial r} + \frac{1}{r} \frac{\partial \varphi_z}{\partial \theta} - \frac{\partial \varphi_\theta}{\partial z}, \quad V_\theta = \frac{1}{r} \frac{\partial \phi}{\partial \theta} + \frac{\partial \varphi_r}{\partial z} - \frac{\partial \varphi_z}{\partial r}, \quad V_z = \frac{\partial \phi}{\partial z} + \frac{1}{r} \frac{\partial (\varphi_\theta r)}{\partial r} - \frac{1}{r} \frac{\partial \varphi_r}{\partial \theta}, \quad (2-4)$$

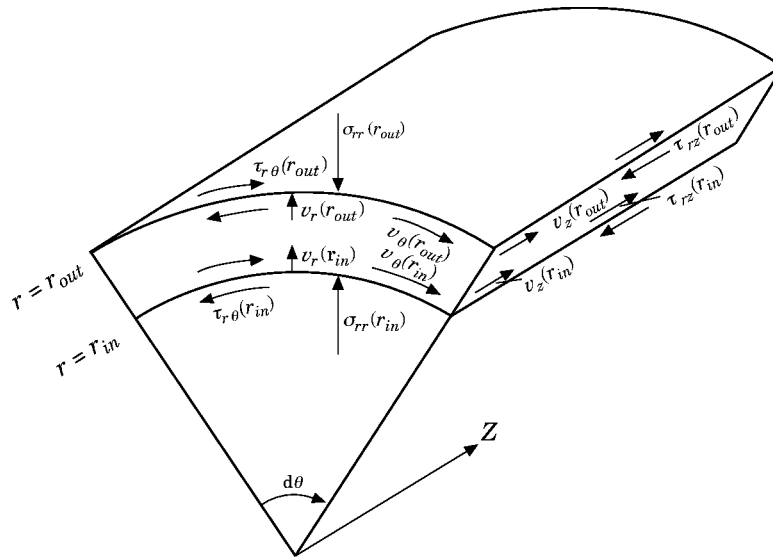


Figure 2. Co-ordinates and state variables on the outside and inside of one layer of the multi-layered cylinder.

where ϕ is the scalar potential and $\vec{\phi}$ is the vector potential. $\varphi_r, \varphi_\theta, \varphi_z$ represent components of the vector potential $\vec{\phi}$. The radial stress σ_{rr} and shear stresses $\tau_{r\theta}$ and τ_{rz} are given by [13]

$$\sigma_{rr} = -\frac{2G}{j\omega} \left\{ \frac{\partial V_r}{\partial r} + \frac{\mu}{1-2\mu} \left(\frac{\partial V_r}{\partial r} + \frac{V_r}{r} + \frac{1}{r} \frac{\partial V_\theta}{\partial \theta} + \frac{\partial V_z}{\partial z} \right) \right\}, \quad (5)$$

$$\tau_{r\theta} = -\frac{G}{j\omega} \left(\frac{\partial V_\theta}{\partial r} - \frac{V_\theta}{r} + \frac{1}{r} \frac{\partial V_r}{\partial \theta} \right), \quad \tau_{rz} = -\frac{G}{j\omega} \left(\frac{\partial V_r}{\partial z} + \frac{\partial V_z}{\partial r} \right), \quad (6, 7)$$

where G denotes the shear modulus, μ the Poisson's ratio, ω the circular frequency of excitation. Substituting equations (2–4) in equations (5–7) yields

$$\sigma_{rr} = -\frac{2G}{j\omega} \left\{ \frac{\partial^2 \phi}{\partial r^2} + \frac{1}{r} \frac{\partial^2 \varphi_z}{\partial r \partial \theta} - \frac{1}{r^2} \frac{\partial \varphi_z}{\partial \theta} - \frac{\partial^2 \varphi_\theta}{\partial r \partial z} + \frac{\mu}{1-2\mu} \left(\frac{\partial^2 \phi}{\partial r^2} + \frac{1}{r} \frac{\partial \phi}{\partial r} + \frac{1}{r^2} \frac{\partial^2 \phi}{\partial \theta^2} + \frac{\partial^2 \phi}{\partial z^2} \right) \right\}, \quad (8)$$

$$\tau_{r\theta} = -\frac{G}{j\omega} \left\{ 2 \left(\frac{1}{r} \frac{\partial^2 \phi}{\partial r \partial \theta} - \frac{1}{r^2} \frac{\partial \phi}{\partial \theta} \right) - \frac{\partial^2 \varphi_z}{\partial r^2} + \frac{1}{r} \frac{\partial \varphi_z}{\partial r} + \frac{1}{r^2} \frac{\partial^2 \varphi_z}{\partial \theta^2} + \frac{\partial^2 \varphi_r}{\partial r \partial z} - \frac{1}{r} \frac{\partial \varphi_r}{\partial z} - \frac{1}{r} \frac{\partial^2 \varphi_\theta}{\partial \theta \partial z} \right\}, \quad (9)$$

$$\tau_{rz} = -\frac{G}{j\omega} \left\{ 2 \frac{\partial^2 \phi}{\partial r \partial z} + \frac{1}{r} \frac{\partial^2 \varphi_z}{\partial z \partial \theta} - \frac{\partial^2 \varphi_\theta}{\partial z^2} + \frac{\partial^2 \varphi_\theta}{\partial r^2} + \frac{1}{r} \frac{\partial \varphi_\theta}{\partial r} - \frac{\varphi_\theta}{r^2} + \frac{1}{r^2} \frac{\partial \varphi_r}{\partial \theta} - \frac{1}{r} \frac{\partial^2 \varphi_r}{\partial r \partial \theta} \right\}. \quad (10)$$

Making use of the equations of motion (136c) of reference [13],

$$G\{(\text{div grad})\vec{V} + [1/(1-2\mu)] \text{grad}(\text{div } \vec{V})\} = \rho \partial^2 \vec{V} / \partial t^2, \quad (11)$$

it can be shown that ϕ and $\varphi_r, \varphi_\theta, \varphi_z$ in equations (2–4) and (8–10) satisfy the wave equations [13]

$$G[2(1-\mu)/(1-2\mu)]\nabla^2 \phi = \rho \partial^2 \phi / \partial t^2, \quad G\nabla^2 \varphi_i = \rho \partial^2 \varphi_i / \partial t^2, \quad i = r, \theta, z, \quad (12a, b)$$

where $\nabla^2 = \partial^2 / \partial r^2 + (1/r) \partial / \partial r + (1/r^2) \partial^2 / \partial \theta^2 + \partial^2 / \partial z^2$ is the Laplacian operator and ρ is the mass density. With the time dependence of all state variables being $e^{i\omega t}$, the space dependence of ϕ and φ_i is given by

$$\nabla^2 \phi + k_L^2 \phi = 0, \quad \nabla^2 \varphi_i + k_T^2 \varphi_i = 0, \quad i = r, \theta, z, \quad (13a, b)$$

where

$$k_L^2 = \left(\frac{\omega}{c_L} \right)^2 = \frac{\omega^2 \rho}{G} \frac{1-2\mu}{2(1-\mu)} = \frac{\omega^2 \rho}{E} \frac{(1-2\mu)(1+\mu)}{(1-\mu)}, \quad k_T^2 = \left(\frac{\omega}{c_T} \right)^2 = \frac{\omega^2 \rho}{G} \quad (14a, b)$$

and subscripts L and T denote longitudinal and transverse shear waves, respectively. c_L , the speed of longitudinal waves, and c_T , the speed of shear waves, are given by

$$c_L^2 = (G/\rho) (2(1-\mu)/(1-2\mu)), \quad c_T^2 = G/\rho. \quad (15)$$

In the outside ambient fluid medium, the incident pressure and scattered pressure can be given by [6]

$$P_i(r, \theta, z, t) = \sum_{n=0}^{\infty} \varepsilon_n (-j)^n J_n(k_{0,y} r) e^{-jk_z z} \cos(n\theta) e^{j\omega t}, \quad (16)$$

$$P_s(r, \theta, z, t) = \sum_{n=0}^{\infty} \varepsilon_n (-j)^n b_n H_n^{(2)}(k_{0,y} r) e^{-jk_z z} \cos(n\theta) e^{j\omega t}. \quad (17)$$

As this paper is concerned with scattering coefficients normalized with respect to the incident wave, the amplitude of the incident wave in equation (16) has been taken to be unity.

The pressure field in the interior fluid of the multi-layered cylinder is given by

$$P_{m+1}(r, \theta, z, t) = \sum_{n=0}^{\infty} \varepsilon_n (-j)^n g_n J_n(k_{m+1,y} r) e^{-jk_z z} \cos(n\theta) e^{j\omega t}. \quad (18)$$

The general solutions of equations (12a, b), for use in the layers of the cylinder, can be written as [6]

$$\phi(r, \theta, z, t) = \sum_{n=0}^{\infty} \varepsilon_n (-j)^n \{A_n J_n(q_L r) + B_n Y_n(q_L r)\} e^{-jk_z z} \cos(n\theta) e^{j\omega t}, \quad (19a)$$

$$\phi_r(r, \theta, z, t) = \sum_{n=0}^{\infty} \varepsilon_n (-j)^n \{C_n J_{n+1}(q_T r) + D_n Y_{n+1}(q_T r)\} e^{-jk_z z} \sin(n\theta) e^{j\omega t}, \quad (19b)$$

$$\phi_\theta(r, \theta, z, t) = \sum_{n=0}^{\infty} -\varepsilon_n (-j)^n \{C_n J_{n+1}(q_T r) + D_n Y_{n+1}(q_T r)\} e^{-jk_z z} \cos(n\theta) e^{j\omega t}, \quad (19c)$$

$$\phi_z(r, \theta, z, t) = \sum_{n=0}^{\infty} \varepsilon_n (-j)^n \{E_n J_n(q_T r) + F_n Y_n(q_T r)\} e^{-jk_z z} \sin(n\theta) e^{j\omega t}, \quad (19d)$$

where $k_0 = \omega/c_0$, $k_{m+1} = \omega/c_{m+1}$, ω is the circular frequency, c_0 and c_{m+1} are the speeds of sound in the exterior and interior ambient fluid media, respectively. $k_{0,y} = k_0 \cos \phi_1$, and $k_z = k_0 \sin \phi_1$ are the wave numbers in the y and z directions in the outside ambient fluid, $k_{m+1,y} = k_{m+1} \cos \phi_2$ is the wave number in the y direction in the inside ambient fluid, q_L and q_T are the wave numbers in the y direction for the longitudinal and shear waves in the layers, respectively. $\varepsilon_n = 1$ for $n = 0$ and $\varepsilon_n = 2$ for $n \geq 1$. Here, $H_n^{(2)} = J_n - jY_n$ is the Hankel function of the second kind for the n th azimuthal mode, J_n and Y_n are Bessel and Neumann functions of order n , respectively. b_n , A_n , B_n , C_n , D_n , E_n , F_n and g_n are the scattering coefficients. The incident and transmitted angles ϕ_1 and ϕ_2 are related by the expression $k_0 \sin \phi_1 = k_{m+1} \sin \phi_2$.

The wave numbers k_L , k_T , k_z , q_L and q_T are related by the compatibility equations

$$q_L^2 = k_L^2 - k_z^2, \quad q_T^2 = k_T^2 - k_z^2. \quad (20a, b)$$

The presence of structural damping represented by a loss factor would make E and G and thence c_L and c_T , k_L and k_T , q_L , and q_T , complex, which would make the arguments of the Bessel functions of all three kinds complex. The general relationships that are

applicable to the Bessel functions with complex arguments [12] are used in the derivations presented here.

Evaluation of the scattering coefficients b_n and g_n , and the level difference or noise reduction, represent formulation of the present problem.

3. DERIVATION OF THE TRANSFER MATRIX

Substituting equations (19a–d) in equations (2–4) and (8–10) yields the state variables σ_{rr} , $\tau_{r\theta}$, τ_{rz} , V_z , V_r and V_θ for the first layer in terms of the constants A_n , B_n , C_n , D_n , E_n and F_n on the inside and outside radii of the first layer.

Defining the identities

$$\alpha_{n,1} \equiv A_n J_n(q_L r) + B_n Y_n(q_L r), \quad \alpha_{n,2} \equiv A_n J_n(q_L r) + B_n Y'_n(q_L r), \quad (21a, b)$$

$$\beta_{n,1} \equiv C_n J_{n+1}(q_T r) + D_n Y_{n+1}(q_T r), \quad \beta_{n,2} \equiv C_n J'_{n+1}(q_T r) + D_n Y'_{n+1}(q_T r), \quad (22a, b)$$

$$\delta_{n,1} \equiv E_n J_n(q_T r) + F_n Y_n(q_T r), \quad \delta_{n,2} \equiv E_n J'_n(q_T r) + F_n Y'_n(q_T r), \quad (23a, b)$$

one can write the state variables as

$$V_r = \sum_{n=0}^{\infty} \varepsilon_n (-j)^n \left(q_L \alpha_{n,2} + \frac{n}{r} \delta_{n,1} - jk_z \beta_{n,1} \right) \exp(-jk_z z) \cos(n\theta), \quad (24)$$

$$V_\theta = \sum_{n=0}^{\infty} \varepsilon_n (-j)^n \left(-\frac{n}{r} \alpha_{n,1} - q_T \delta_{n,2} - jk_z \beta_{n,1} \right) \exp(-jk_z z) \sin(n\theta), \quad (25)$$

$$V_z = \sum_{n=0}^{\infty} -\varepsilon_n (-j)^n \left(jk_z \alpha_{n,1} + \frac{n+1}{r} \beta_{n,1} + q_T \beta_{n,2} \right) \exp(-jk_z z) \cos(n\theta), \quad (26)$$

$$\begin{aligned} \sigma_{rr} = & \sum_{n=0}^{\infty} -\varepsilon_n (-j)^n \frac{2G}{j\omega} \left[\left\{ k_z^2 - \frac{k_T^2}{2} \left(1 - \frac{F}{r^2} \right) \right\} \alpha_{n,1} - \frac{q_L}{r} \alpha_{n,2} - \frac{n}{r^2} \delta_{n,1} + \frac{n}{r} q_T \delta_{n,2} - jk_z q_T \beta_{n,2} \right] \\ & \times \exp(-jk_z z) \cos(n\theta), \end{aligned} \quad (27)$$

$$\begin{aligned} \tau_{r\theta} = & \sum_{n=0}^{\infty} -\varepsilon_n (-j)^n \frac{2G}{j\omega} \left[\frac{n}{r^2} \alpha_{n,1} - \frac{n}{r} q_L \alpha_{n,2} + \frac{q_T}{r} \delta_{n,2} + \left\{ \frac{q_T^2}{2} - \frac{n^2}{r^2} \right\} \delta_{n,1} \right. \\ & \left. + \frac{jk_z}{2} \left\{ \frac{n+1}{r} \beta_{n,1} - q_T \beta_{n,2} \right\} \right] \exp(-jk_z z) \sin(n\theta), \end{aligned} \quad (28)$$

$$\begin{aligned} \tau_{rz} = & \sum_{n=0}^{\infty} -\varepsilon_n (-j)^n \frac{G}{j\omega} \left[-jk_z \left\{ 2q_L \alpha_{n,2} + \frac{n}{r} \delta_{n,1} \right\} + \left\{ k_T^2 - 2k_z^2 - \frac{n^2}{r^2} + \frac{n+1}{r^2} \right\} \beta_{n,1} - \frac{nq_T}{r} \beta_{n,2} \right] \\ & \times \exp(-jk_z z) \cos(n\theta), \end{aligned} \quad (29)$$

where

$$F = 2n^2/k_T^2. \quad (30)$$

The modal equations of the state variables can be written as

$$V_{r,n} = (q_L \alpha_{n,2} + (n/r)\delta_{n,1} - jk_z \beta_{n,1}) \exp(-jk_z z), \quad (31)$$

$$V_{\theta,n} = -((n/r)\alpha_{n,1} + q_T \delta_{n,2} + jk_z \beta_{n,1}) \exp(-jk_z z), \quad (32)$$

$$V_{z,n} = -\left(jk_z \alpha_{n,1} + \frac{n+1}{r} \beta_{n,1} + q_T \beta_{n,2}\right) \exp(-jk_z z), \quad (33)$$

$$\begin{aligned} \sigma_{rr,n} = & -\frac{2G}{j\omega} \left[\left\{ k_z^2 - \frac{k_T^2}{2} \left(1 - \frac{F}{r^2} \right) \right\} \alpha_{n,1} - \frac{q_L}{r} \alpha_{n,2} - \frac{n}{r^2} \delta_{n,1} + \frac{n}{r} q_T \delta_{n,2} - jk_z q_T \beta_{n,2} \right] \\ & \times \exp(-jk_z z), \end{aligned} \quad (34)$$

$$\begin{aligned} \tau_{r\theta,n} = & -\frac{2G}{j\omega} \left[\frac{n}{r^2} \alpha_{n,1} - \frac{n}{r} q_L \alpha_{n,2} + \frac{q_T}{r} \delta_{n,2} + \left\{ \frac{q_T^2}{2} - \frac{n^2}{r^2} \right\} \delta_{n,1} + \frac{jk_z}{2} \left\{ \frac{n+1}{r} \beta_{n,1} - q_T \beta_{n,2} \right\} \right] \\ & \times \exp(-jk_z z), \end{aligned} \quad (35)$$

$$\begin{aligned} \tau_{rz,n} = & -\frac{G}{j\omega} \left[-jk_z \left\{ 2q_L \alpha_{n,2} + \frac{n}{r} \delta_{n,1} \right\} + \left\{ k_T^2 - 2k_z^2 - \frac{n^2}{r^2} + \frac{n+1}{r^2} \right\} \beta_{n,1} - \frac{nq_T}{r} \beta_{n,2} \right] \\ & \times \exp(-jk_z z). \end{aligned} \quad (36)$$

The modal equations (31–36) can now be used to write expressions (24–29) of the state variables in the simplified forms

$$V_r = \sum_{n=0}^{\infty} \varepsilon_n (-j)^n V_{r,n} \cos(n\theta), \quad V_{\theta} = \sum_{n=0}^{\infty} \varepsilon_n (-j)^n V_{\theta,n} \sin(n\theta), \quad (37, 38)$$

$$V_z = \sum_{n=0}^{\infty} \varepsilon_n (-j)^n V_{z,n} \cos(n\theta), \quad (39)$$

$$\sigma_{rr} = \sum_{n=0}^{\infty} \varepsilon_n (-j)^n \sigma_{rr,n} \cos(n\theta), \quad \tau_{r\theta} = \sum_{n=0}^{\infty} \varepsilon_n (-j)^n \tau_{r\theta,n} \sin(n\theta), \quad (40, 41)$$

$$\tau_{rz} = \sum_{n=0}^{\infty} \varepsilon_n (-j)^n \tau_{rz,n} \cos(n\theta). \quad (42)$$

For the n th azimuthal mode, solving equations (31–36) yields

$$\alpha_{n,1} = f_1 \sigma_{rr,n} + f_2 \tau_{r\theta,n} + f_3 \tau_{rz,n} + f_4 V_{z,n} + f_5 V_{\theta,n} + f_6 V_{r,n}, \quad (43)$$

$$\alpha_{n,2} = g_1 \sigma_{rr,n} + g_2 \tau_{r\theta,n} + g_3 \tau_{rz,n} + g_4 V_{z,n} + g_5 V_{\theta,n} + g_6 V_{r,n}, \quad (44)$$

$$\beta_{n,1} = p_1 \sigma_{rr,n} + p_2 \tau_{r\theta,n} + p_3 \tau_{rz,n} + p_4 V_{z,n} + p_5 V_{\theta,n} + p_6 V_{r,n}, \quad (45)$$

$$\beta_{n,2} = t_1 \sigma_{rr,n} + t_2 \tau_{r\theta,n} + t_3 \tau_{rz,n} + t_4 V_{z,n} + t_5 V_{\theta,n} + t_6 V_{r,n}, \quad (46)$$

$$\delta_{n,1} = h_1 \sigma_{rr,n} + h_2 \tau_{r\theta,n} + h_3 \tau_{rz,n} + h_4 V_{z,n} + h_5 V_{\theta,n} + h_6 V_{r,n}, \quad (47)$$

$$\delta_{n,2} = l_1 \sigma_{rr,n} + l_2 \tau_{r\theta,n} + l_3 \tau_{rz,n} + l_4 V_{z,n} + l_5 V_{\theta,n} + l_6 V_{r,n}. \quad (48)$$

The coefficients f_i, g_i, p_i, t_i, h_i and $l_i, i = 1-6$ in equations (43–48) are given in the Appendix.

By making use of the recurrence relations of Bessel functions, the constants A_n, B_n, C_n, D_n, E_n and F_n can be obtained by solving simultaneously the system of equations (43–48). Substituting these values of the constants A_n, B_n, C_n, D_n, E_n and F_n in the expressions of state variables at $r = r_{out}$ given by equations (31–36), (the rather lengthy but straightforward algebraic details are omitted here), one obtains the following transfer matrix relationship between the state vector at (r_{out}, θ, z, n) and that at (r_{in}, θ, z, n) :

$$\begin{bmatrix} \sigma_{rr,n}(r_{out}) \\ \tau_{r\theta,n}(r_{out}) \\ \tau_{rz,n}(r_{out}) \\ V_{z,n}(r_{out}) \\ V_{\theta,n}(r_{out}) \\ V_{r,n}(r_{out}) \end{bmatrix} = \begin{bmatrix} A_{11} & A_{12} & A_{13} & A_{14} & A_{15} & A_{16} \\ A_{21} & A_{22} & A_{23} & A_{24} & A_{25} & A_{26} \\ A_{31} & A_{32} & A_{33} & A_{34} & A_{35} & A_{36} \\ A_{41} & A_{42} & A_{43} & A_{44} & A_{45} & A_{46} \\ A_{51} & A_{52} & A_{53} & A_{54} & A_{55} & A_{56} \\ A_{61} & A_{62} & A_{63} & A_{64} & A_{65} & A_{66} \end{bmatrix} \begin{bmatrix} \sigma_{rr,n}(r_{in}) \\ \tau_{r\theta,n}(r_{in}) \\ \tau_{rz,n}(r_{in}) \\ V_{z,n}(r_{in}) \\ V_{\theta,n}(r_{in}) \\ V_{r,n}(r_{in}) \end{bmatrix}. \quad (49)$$

The elements A_{ij} of this transfer matrix are given in the Appendix.

4. EVALUATION OF SCATTERING AND TRANSMISSION COEFFICIENTS OF MULTI-LAYERED CYLINDER WITH TWO-DIMENSIONAL PRESSURE EXCITATION

The procedure used in deriving the transfer matrix relation (49) for the first layer can be made use of in deriving the transfer matrices of the successive layers 2 to m as well. Then the multi-layer system, comprising the exterior ambient medium “0”, m successive layers and the interior medium “ $m + 1$ ”, can be represented by an overall transfer matrix, as given by

$$[S]_0 = [A] [S]_m, \quad (50)$$

where

$$[A] = [A]_1 [A]_2 \dots [A]_m. \quad (51)$$

$[A]$, the overall transfer matrix for the n th azimuthal mode, can be written as

$$\begin{bmatrix} \sigma_{rr,0,n} \\ \tau_{r\theta,0,n} \\ \tau_{rz,0,n} \\ V_{z,0,n} \\ V_{\theta,0,n} \\ V_{r,0,n} \end{bmatrix} = \begin{bmatrix} A_{11} & A_{12} & A_{13} & A_{14} & A_{15} & A_{16} \\ A_{21} & A_{22} & A_{23} & A_{24} & A_{25} & A_{26} \\ A_{31} & A_{32} & A_{33} & A_{34} & A_{35} & A_{36} \\ A_{41} & A_{42} & A_{43} & A_{44} & A_{45} & A_{46} \\ A_{51} & A_{52} & A_{53} & A_{54} & A_{55} & A_{56} \\ A_{61} & A_{62} & A_{63} & A_{64} & A_{65} & A_{66} \end{bmatrix} \begin{bmatrix} \sigma_{rr,m,n} \\ \tau_{r\theta,m,n} \\ \tau_{rz,m,n} \\ V_{z,m,n} \\ V_{\theta,m,n} \\ V_{r,m,n} \end{bmatrix}. \quad (52)$$

The ambient media in contact with layers 1 and m being fluids, shear stresses on both the exposed surfaces of the multi-layer system will be zero: i.e.,

$$\tau_{r\theta,0,n} = \tau_{r\theta,m,n} = \tau_{rz,0,n} = \tau_{rz,m,n} = 0. \quad (53)$$

The modal pressure and modal radial velocity on the exterior face are given by

$$P_{0,n} = \{J_n(k_{0,y} r_{out}) + b_n H_n^{(2)}(k_{0,y} r_{out})\} e^{-jk_z z} \cos(n\theta) e^{j\omega t}, \quad (54)$$

$$V_{r,0,n} = (j/\rho_0 c_0) \{J_n'(k_{0,y} r_{out}) + b_n H_n^{(2)'}(k_{0,y} r_{out})\} e^{-jk_z z} \cos(n\theta) e^{j\omega t}. \quad (55)$$

The modal impedance of the incident wave and scattered waves on the exterior surface can be given by

$$Z_{0,n,i} = -j\rho_0 c_0 J_n(k_{0,y} r_{out})/J'_n(k_{0,y} r_{out}), \quad Z_{0,n,s} = -j\rho_0 c_0 H_n^{(2)}(k_{0,y} r_{out})/H_n^{(2)'}(k_{0,y} r_{out}). \quad (56, 57)$$

The standing wave pressure is equal to the normal compressive stress: i.e.,

$$\sigma_{rr,0,n} = P_{0,n}. \quad (58)$$

The corresponding relationships for the interior face are

$$P_{m,n} = g_n J_n(k_{m+1,y} r_{in}) e^{-jk_z z} \cos(n\theta), \quad V_{r,m,n} = \frac{jg_n J'_n(k_{m+1,y} r_{in})}{\rho_{m+1} c_{m+1}} e^{-jk_z z} \cos(n\theta), \quad (59, 60)$$

$$Z_{m+1,n} = -j\rho_{m+1} c_{m+1} J_n(k_{m+1,y} r_{in})/J'_n(k_{m+1,y} r_{in}), \quad \sigma_{rr,m,n} = P_{m,n} = V_{r,m,n} Z_{m+1,n} \quad (61, 62)$$

where $Z_{m+1,n}$ is the modal impedance exerted on the interior surface. The function $e^{-jk_z z} \cos(n\theta) e^{j\omega t}$ is common for modal pressure and modal radial velocity on both the exterior and interior faces, and therefore can be dropped henceforth for convenience of writing.

Making use of the boundary conditions (53), (54), (58) and (62), and the transfer matrix (49), one obtains

$$V_{r,m,n} = -(P_{0,n}/DEN)A_{25}, \quad V_{\theta,m,n} = -(P_{0,n}/A_{15})\{1 + [A_{25}(M_{11} - A_{14}M_{35})/DEN]\}, \quad (63, 64)$$

$$V_{z,m,n} = -V_{r,m,n}M_{35} = (A_{25}/DEN)P_{0,n}M_{35}, \quad V_{r,0,n}\zeta = P_{0,n}, \quad (65, 66)$$

where

$$DEN = A_{15}\{M_{21} - M_{35}A_{24} - M_{11}A_{25}/A_{15} + M_{35}A_{14}A_{25}/A_{15}\}, \quad (67)$$

$$M_{11} = A_{11}Z_{m+1} + A_{16}, \quad M_{21} = A_{21}Z_{m+1} + A_{26}, \quad M_{31} = A_{31}Z_{m+1} + A_{36}, \quad (68a-c)$$

$$M_{35} = (A_{35}M_{21} - A_{25}M_{31})/(A_{35}A_{24} - A_{25}A_{34}), \quad M_{61} = A_{61}Z_{m+1} + A_{66}. \quad (68d, e)$$

ζ in equation (66) represents the equivalent impedance of the complete passive sub-system consisting of layers 1 to m (whose impedance is denoted by ζ_L) and the radiation impedance exerted by the interior ambient fluid medium $m+1$ (whose impedance is denoted by Z_{m+1}).

The equivalent impedance $\zeta = f(\zeta_L, Z_{m+1})$ is given by

$$\zeta = \frac{\{A_{15}M_{21} - A_{15}M_{35}A_{24} - M_{11}A_{25} + M_{35}A_{14}A_{25}\}}{\{-A_{25}M_{61} + A_{25}A_{64}M_{35} + A_{65}M_{21} - A_{24}A_{65}M_{35}\}}. \quad (69)$$

Substituting equations (54) and (55) into equation (66) yields an expression for the scattering coefficient b_n :

$$b_n = \{\rho_0 c_0 J_n(k_{0,y} r_{out}) - j\zeta J'_n(k_{0,y} r_{out})\}/\{j\zeta H_n^{(2)'}(k_{0,y} r_{out}) - \rho_0 c_0 H_n^{(2)}(k_{0,y} r_{out})\}. \quad (70)$$

By making use of the expressions for the modal incident and scattered wave impedances and surface impedances on the interior surface given in equations (56), (57) and (61), one can write equation (70) as

$$b_n = -[J'_n(k_{0,y} r_{out})/H_n^{(2)'}(k_{0,y} r_{out})][(\zeta - Z_{0,n,i})/(\zeta - Z_{0,n,s})]. \quad (71)$$

Substitution of expression (71) for the scattering coefficient into equation (17) yields the expression for the scattered pressure:

$$P_s = \sum_{n=0}^{\infty} -\varepsilon_n (-j)^n \frac{J_n'(k_{0,y} r_{out})}{H_n^{(2)'}(k_{0,y} r_{out})} \frac{(\zeta - Z_{0,n,i})}{(\zeta - Z_{0,n,s})} H_n^{(2)}(k_{0,y} r_{out}) \exp(-jk_z z) \cos(n\theta). \quad (72)$$

In the far field, by making use of the asymptotic representation for the Hankel function of the second kind given in reference [14],

$$H_n^{(2)} = (2/\pi k_{0,y} r)^{0.5} \exp(-j(k_{0,y} r - n\pi/2 - \pi/4)), \quad (73)$$

the scattered pressure defined in equation (72) can be written as

$$P_s = \left(\frac{2j}{\pi k_{0,y} r_{out}} \right)^{0.5} \exp(-jk_{0,y} r_{out}) \exp(-jk_z z) \sum_{n=0}^{\infty} \varepsilon_n b_n \cos(n\theta). \quad (74)$$

The scattering form function is defined as [6]

$$|f_{\infty}| = \frac{2}{(\pi k_{0,y} r_{out})^{0.5}} \left| \sum_{n=0}^{\infty} \varepsilon_n b_n \cos(n\theta) \right|. \quad (75)$$

For the case of monostatic back scattering, $\theta = \pi$, making $\cos(n\pi) = (-1)^n$, the expression for the scattering form function becomes

$$|f_{\infty}| = \frac{2}{(\pi k_{0,y} r_{out})^{0.5}} \left| \sum_{n=0}^{\infty} \varepsilon_n b_n (-1)^n \right|. \quad (76)$$

Upon substituting expression (54) for the scattering coefficient b_n into equation (76), and making use of equations (59–62), one finds

$$g_n = \{J_n(k_{0,y} r_{out}) + b_n H_n^{(2)}(k_{0,y} r_{out})\} A_{25} Z_{m+1} / DEN J_n(k_{m+1,y} r_{in}). \quad (77)$$

Substitution of this expression into equation (18) yields the pressure field transmitted through the shell:

$$P_{m+1} = \sum_{n=0}^{\infty} \varepsilon_n (-j)^n \{J_n(k_{0,y} r_{out}) + b_n H_n^{(2)}(k_{0,y} r_{out})\} \frac{A_{25} Z_{m+1,n}}{DEN} \exp(-jk_z z) \cos(n\theta). \quad (78)$$

The level difference, or noise reduction, achieved by the cylindrical shell is given by

$$\begin{aligned} NR &= 20 \log_{10} \left| \frac{(P_i + P_s)}{P_{m+1}} \right| \\ &= 20 \log_{10} \left[\frac{\sum_{n=0}^{\infty} \varepsilon_n (-j)^n \{J_n(k_{0,y} r_{out}) + b_n H_n^{(2)}(k_{0,y} r_{out})\} \exp(-jk_z z) \cos(n\theta)}{\sum_{n=0}^{\infty} \varepsilon_n (-j)^n g_n J_n(k_{m+1,y} r_{in}) \exp(-jk_{in} z) \cos(n\theta)} \right]. \end{aligned} \quad (79)$$

For the case of monostatic back scattering, $\theta = \pi$, making $\cos(n\pi) = (-1)^n$, the expression for noise reduction becomes

$$NR = 20 \log_{10} \left| \frac{(P_i + P_s)}{P_{m+1}} \right|$$

$$= 20 \log_{10} \left[\frac{\sum_{n=0}^{\infty} \varepsilon_n (-j)^n \{J_n(k_{0,y} r_{out}) + b_n H_n^{(2)}(k_0 r_{out})\} \exp(-jk_z z) (-1)^n}{\sum_{n=0}^{\infty} \varepsilon_n (-j)^n F_n J_n(k_{m+1,y} r_{in}) \exp(-jk_z z) (-1)^n} \right]. \quad (80)$$

In the limiting case of one-dimensional pressure excitation, the expressions for $V_{r,m,n}$, $V_{\theta,m,n}$, DEN , b_n and g_n , given in equations (63), (64), (67), (70) and (77), become

$$V_{r,m,n} = (T_{23}/DEN)P_{0,n}, \quad V_{\theta,m,n} = -(T_{21} Z_{m+1} + T_{24})P_{0,n}/DEN, \quad (81, 82)$$

$$DEN = -T_{13}(T_{21} Z_{m+1} + T_{24}) + T_{23}(T_{11} Z_{m+1} + T_{14}), \quad (83)$$

$$b_n = \{\rho_0 c_0 J_n(k_{0,y} r_{out}) - j\zeta J'_n(k_{0,y} r_{out})\} / \{j\zeta H_n^{(2)'}(k_{0,y} r_{out}) - \rho_0 c_0 H_n^{(2)}(k_{0,y} r_{out})\}, \quad (84)$$

where

$$\zeta = \{T_{23}(T_{11} Z_{m+1,n} + T_{14}) - T_{13}(T_{21} Z_{m+1,n} + T_{24})\} / \{T_{23}(T_{41} Z_{m+1,n} + T_{44}) - T_{43}(T_{21} Z_{m+1,n} + T_{24})\}, \quad (85a)$$

$$g_n = \{J_n(k_{0,y} r_{out}) + b_n H_n^{(2)}(k_{0,y} r_{out})\} \frac{T_{23} Z_{m+1}}{DEN J_n(k_{m+1,y} r_{in})}. \quad (85b)$$

Here the following equivalences of the elements of the 6×6 transfer matrix $[A]_{ij}$ of equation (49) in the limiting case of one-dimensional pressure excitation to elements of the 4×4 transfer matrix $[T]_{ij}$ in reference [10] have been used:

$$A_{15} = T_{13}, \quad A_{16} = T_{14}, \quad A_{25} = T_{23}, \quad A_{26} = T_{24}, \quad (86a)$$

$$M_{11} = A_{11} Z_{m+1} + A_{16} = T_{11} Z_{m+1} + A_{14}, \quad M_{21} = A_{21} Z_{m+1} + A_{26} = T_{21} Z_{m+1} + T_{24}, \quad (86b, c)$$

$$M_{31} = A_{31} Z_{m+1} + A_{36} \text{ vanishes}, \quad (86d)$$

$$M_{35} = (A_{35} M_{21} - A_{25} M_{31}) / (A_{35} A_{24} - A_{25} A_{34}) \text{ vanishes}, \quad (86e)$$

$$M_{61} = A_{61} Z_{m+1} + A_{66} = T_{41} Z_{m+1} + T_{44}. \quad (86f)$$

It may be seen that equations (81–85) are identical to equations (62–64), (69) and (77), respectively, in reference [10]. These deductions confirm that the expressions of scattering coefficient and noise reduction given above in equations (70) and (79) for the case of two-dimensional pressure excitation embody in them the one-dimensional or normal pressure excitation dealt with in reference [10].

5. RESPONSE OF THE MULTI-LAYERED CYLINDER TO EXTERNAL EXCITATION

The transfer matrix relation (49) can be used to evaluate the radial velocities at the two exposed surfaces of the multi-layer cylinder excited by a two-dimensional pressure

excitation, or alternatively to evaluate the acoustic pressure distribution excited by the radial velocity components of the radiating surfaces.

Let the modal external excitation on the exterior of the first layer have the following distribution:

$$P_{0,n} = \{J_n(k_{0,y} r_{out}) + b_n H_n^{(2)}(k_{0,y} r_{out})\} \exp(-jk_z z) \cos(n\theta). \quad (87)$$

The resulting compressive stresses at the exposed surfaces $r = r_{in}$ and $r = r_{out}$ are given by

$$\sigma_{rr,n,0} = P_{0,n} - Z_{0,n} V_{r,0,n}, \quad \sigma_{rr,n,m} = Z_{m+1,n} V_{r,m,n}, \quad (88, 89)$$

where $Z_{0,n}$ and $Z_{m+1,n}$ are the modal radiation impedances exerted by the ambient medium in contact with the first layer and the m th layer, respectively (see equations (56), (57) and (61)).

If the ambient media are fluids, they will not support any shear stresses. Then,

$$\tau_{r\theta,0,n} = \tau_{r\theta,m,n} = \tau_{rz,0,n} = \tau_{rz,m,n} = 0. \quad (90)$$

Substituting the six boundary conditions (88–90) in the six equations of the transfer matrix (49), one can derive the expressions for the normal velocities at the two exposed surfaces. With the algebraic details omitted, one finds

$$V_{\theta,m,n} = \frac{P_{0,n} - \{M_{11} - A_{14} M_{35} + Z_{0,n} (M_{61} - A_{64} M_{35})\}}{(A_{15} + Z_{0,n} A_{65})} V_{r,m,n}, \quad (91)$$

$$V_{r,m,n} = (A_{25} / DEN) P_{0,n}, \quad (92)$$

$$V_{r,0,n} = \left\{ \frac{A_{65}}{(A_{65} Z_{0,n} + A_{15})} - \frac{A_{25} (M_{11} A_{65} - A_{14} M_{35} A_{65} - M_{61} A_{15} + A_{64} M_{35} A_{15})}{DEN (A_{65} Z_{0,n} + A_{15})} \right\}, \quad (93)$$

where

$$DEN = -(A_{15} + Z_{0,n} A_{65}) (M_{21} - A_{24} M_{35}) + A_{25} \{M_{11} - A_{14} M_{35} + Z_{0,n} (M_{61} - A_{64} M_{35})\}. \quad (94)$$

Incidentally, in the limiting case of one-dimensional pressure excitation, $V_{r,m,n}$, $V_{r,0,n}$ and DEN given by equations (92–94) turn out to be

$$V_{r,m,n} = \frac{T_{23}}{\{-M_{21} (T_{13} + Z_{0,n} T_{43}) + T_{23} (M_{11} + Z_{0,n} M_{41})\}} P_{0,n}, \quad (95)$$

$$V_{r,0,n} = \left\{ T_{43} - \frac{T_{23} (T_{43} M_{11} - T_{13} M_{41})}{DEN} \right\} \frac{P_{0,n}}{(T_{13} + Z_{0,n} T_{43})}, \quad (96)$$

$$DEN = \{-(T_{43} Z_{0,n} + T_{13}) M_{21} + (M_{41} Z_{0,n} + M_{11}) T_{23}\}. \quad (97)$$

Equations (95–97) may be seen to tally with the corresponding expressions (96), (99) and (97), respectively, in reference [10], thereby confirming that expressions (92–94) reduce to those for the normal or one-dimensional pressure excitation in the limiting case.

6. NUMERICAL RESULTS

In order to illustrate the use of this transfer matrix approach to evaluate the scattering coefficient and noise reduction of a two-layer infinite cylinder, for the case of oblique incidence and two-dimensional pressure excitation, some numerical examples are

TABLE 1
Material properties

Material	Density (ρ)	Modulus of elasticity (E)	Poisson's ratio (μ)
Elastomer layer	1200	$3.3 \times 10^8 (1 + j0.8)$	0.49
Backing steel layer	7800	$2.1 \times 10^{11}(1 + j0.002)$	0.31

presented. Unless otherwise specified, the configuration chosen is a carbon steel infinite cylinder of 5 mm thickness ($r_{out} = 100$ mm, $r_{in} = 95$ mm). Results are shown for the frequency range of $k_0 r_{out} = 0-20$, which is typical of the underwater acoustic applications for which the present model is primarily expected to be used. Default values of the outer and inner radius of the multi-layer cylinder consisting of a carbon steel inner cylinder lined with an outer elastomer cylindrical layer are $r_{out} = 100$ mm and $r_{in} = 90$ mm ($r_{out} = 100$ mm and $r_{in} = 95$ mm for the elastomer cylinder, and $r_{out} = 95$ mm and $r_{in} = 90$ mm for the steel cylinder). Monostatic back scattering is considered for all the computations. Water and air are considered as the ambient medium outside and inside of the cylinder, respectively.

Values of the density (kg/m^3), Poisson's ratio and elastic modulus (Pa) for the two constituent layers are given in Table 1.

The presence of structural damping represented by a loss factor would make E and G and thence c_L and c_T , or k_L and k_T , complex, which would make the arguments of the Bessel functions of all three kinds complex. The series representations for Bessel functions [14] are used in the computations.

Values of the density (kg/m^3) and speed of sound (m/s) for sea water and air (which are the ambient media) are given in Table 2.

Figure 3 shows the scattering form function plotted for the case of the aluminium cylinder ($r_{out} = 100$ mm, $r_{in} = 95$ mm) as calculated by using the present transfer matrix method for three different angles of incidence ϕ_1 (0° , 9° and 24°). It is observed through the numerical computation that the values of scattering form function obtained for this case by using the normal solution of reference [6], and by the present method, agree to the fourth decimal, which indeed indicates that both the methods lead to the same result, confirming the validity of the matrix elements presented in the Appendix.

Figures 4 and 5 show the effect of the angle of incidence ϕ_1 on the scattering form function and noise reduction, plotted for the case of a steel cylinder ($r_{out} = 100$ mm and $r_{in} = 95$ mm). The angle of incidence is chosen to cover all the four cases of interest: i.e., $\phi_1 = 0$, $\phi_1 < \phi_{1,L}$, $\phi_{1,L} < \phi_1 < \phi_{1,T}$ and $\phi_1 > \phi_{1,T}$, where $\phi_{1,L}$ and $\phi_{1,T}$ are the values of the critical angle for longitudinal waves and transverse waves, respectively. It can be observed from Figure 4 that the trends of $|f_\infty|$ for $\phi_1 = 0^\circ$ and $\phi_1 = 10^\circ$ look alike except for a shift of the peaks to the lower side of the frequency for the latter case. The plot for the case of $\phi_1 = 30^\circ$ contains rapid kinks at higher frequencies which are due to incidence beyond the critical angle.

TABLE 2
Ambient media properties

Ambient medium	Density (ρ)	Speeds of sound (c_0)
Sea Water	1025	1500
Air	1.18	340

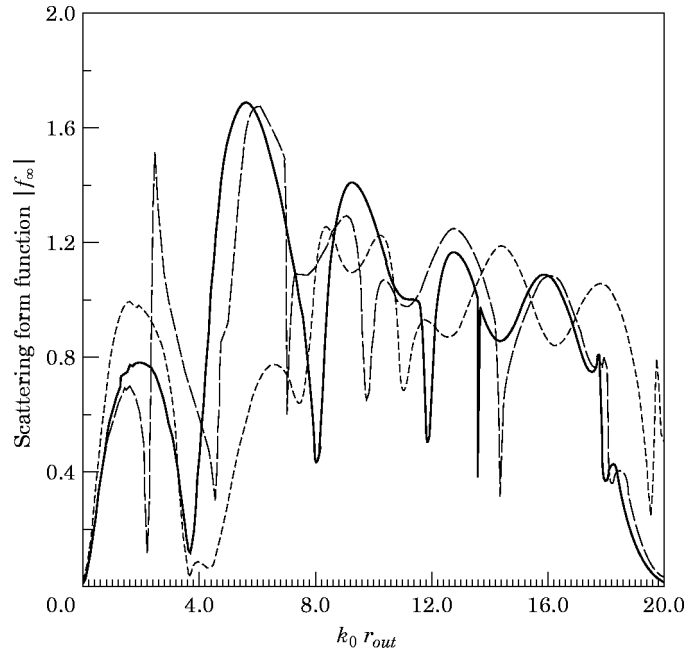


Figure 3. Scattering form functions $|f_\infty|$ for aluminium cylinder compared with normal mode solution of reference [6] for various angles of incidence ϕ_1 . —, 0° ; ----, 9° ; ····, 24° .

Figures 6 and 7 show the scattering form function and noise reduction for various layer configurations. Results are plotted for the cases of an elastomer cylinder ($r_{out} = 100$ mm and $r_{in} = 95$ mm), steel cylinder ($r_{out} = 100$ mm and $r_{in} = 95$ mm), and the combination of the two (lined cylinder, $r_{out} = 100$ mm and $r_{in} = 90$ mm) for $\phi_1 = 10^\circ$. Results are plotted for $k_0 r_{out} = 0-5$ only for the sake of clarity of observation. It is observed from Figure 6 that there is a sharp peak at about 10 000 Hz ($k_0 r_{out} = 0-5$) for the case of the elastomer cylinder, which is smoothed out by the presence of the backing steel cylinder for the case of the lined cylinder. As expected, the presence of the elastomer layer in a lined cylinder enhances the noise reduction at all frequencies, compared to the case of single steel cylinder, as can be observed from Figure 7.

6.1. FOUR-LAYERED ELASTOMER OR POLYMER HOSE†

There are hoses like those used in automotive climate control systems where the hose wall is made up of four different types of elastomers or polymers. The transfer matrix method can deal with this four-layer cylindrical hose with equal ease. Results are shown in Figures 8 and 9 for two configurations shown in Table 3. The abscissa is $kr_{sh} \equiv k_0 r_{out}$ in both the figures. Each of the four layers in either configuration is 5 mm thick. The outermost radius is 100 mm as for the previous cases. The medium is air on the outside as well as inside.

It may be observed from Figure 8 that reversing the order of the layers has little effect on the scattering form function, where the two curves are completely overlapping. This is typical of the symmetrical nature of impedance mismatch, as shown for sudden expansion and contraction in reference [7] and for change in media in reference [13]. However, the curvature effect of the cylindrical surfaces produces considerable differences

† This example is also presented in reference [10], but is included for completeness here, in response to comments by the referees.

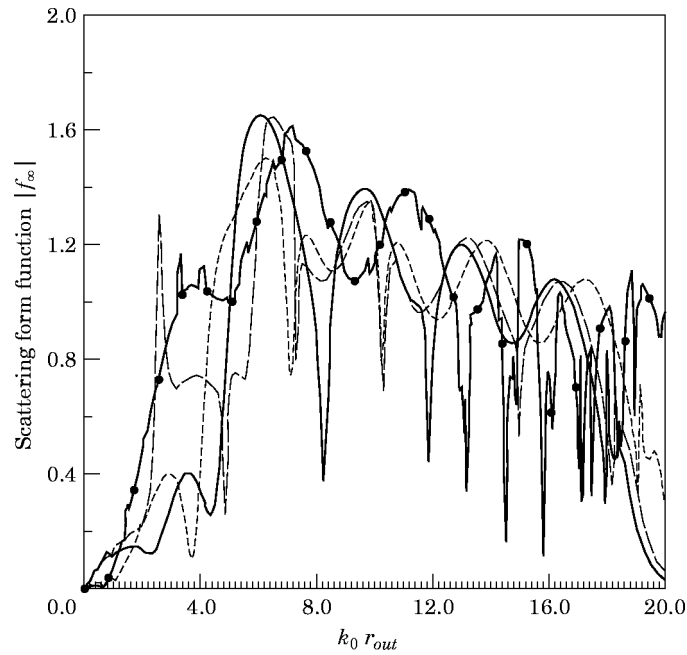


Figure 4. Scattering form functions $|f_\infty|$ of a steel cylinder at various angles of incidence ϕ_i . —, 0° ; ----, 10° ; ···, 20° ; —●—, 30° .

in the noise reduction values as may be noted from Figure 9. This effect has also been observed in the interchange of the rubber and steel layers, although it is not shown here. Nevertheless, the primary purpose of Figures 8 and 9 is to show that the transfer matrix

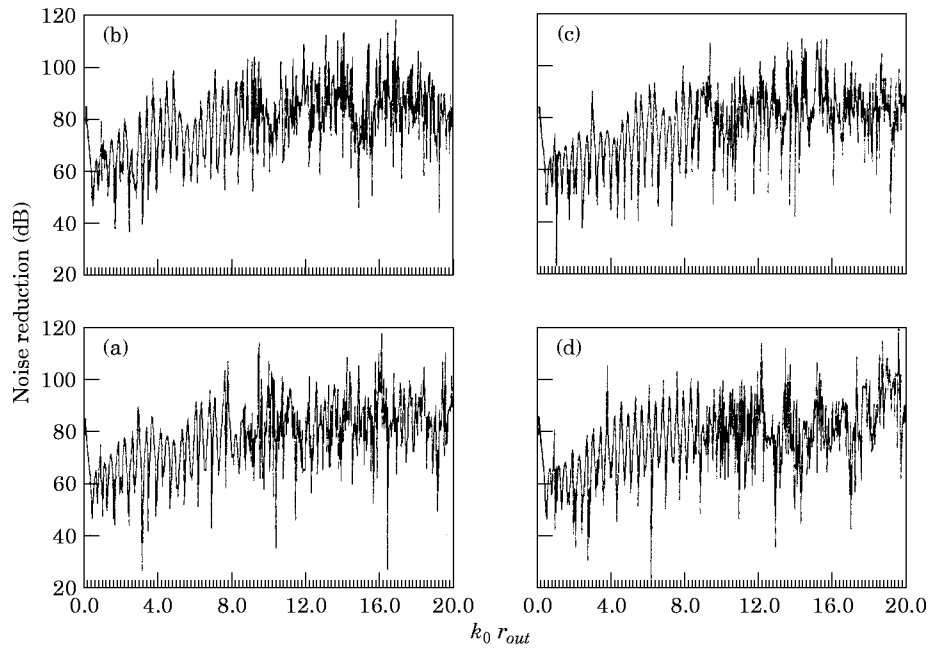


Figure 5. Noise reduction NR of a steel cylinder at various angles of incidence ϕ_i . (a), 0° ; (b), 10° ; (c), 20° ; (d), 30° .

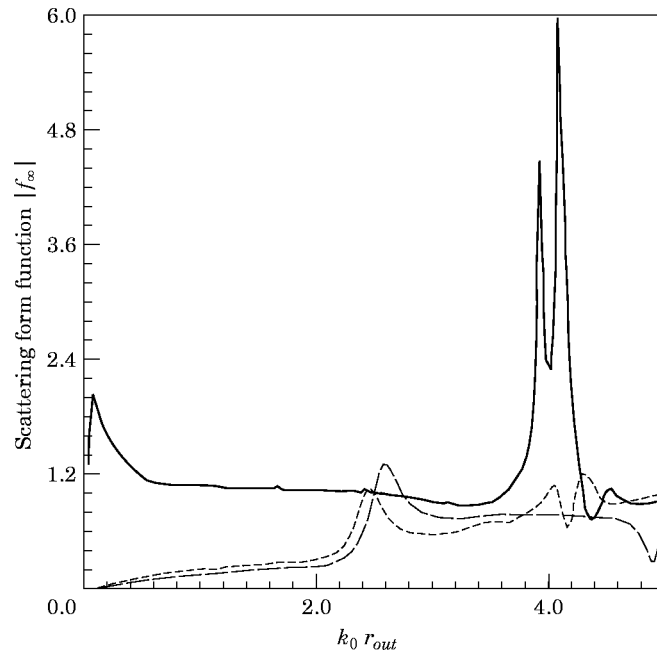


Figure 6. Scattering form functions $|f_\infty|$ for various cylinder configurations. —, Elastomer cylinder alone; ---, backing steel cylinder alone; ····, steel cylinder lined with elastomer layer.

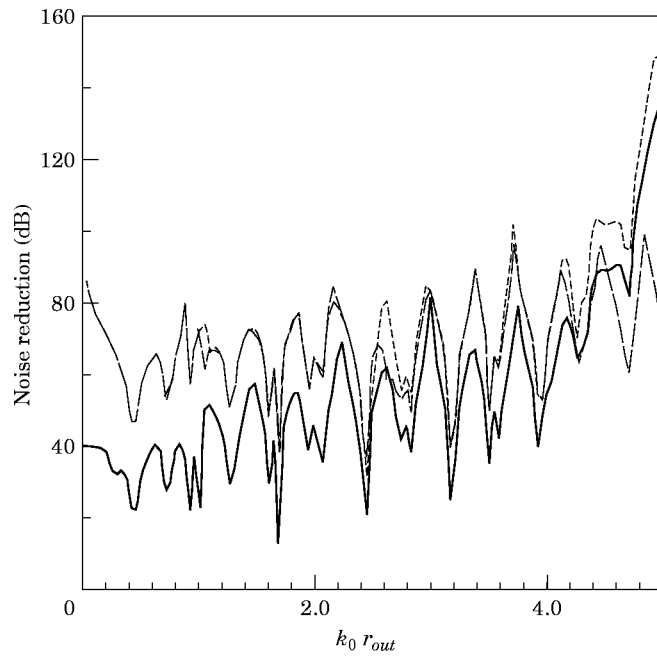


Figure 7. Noise reduction NR for various cylinder configurations. —, Elastomer cylinder alone; ----, backing steel cylinder alone; ····, steel cylinder lined with elastomer layer.

TABLE 3
Hose configurations

	Poisson's ratio μ	Density ρ (km/m ³)	Storage modulus E_r (Pa)	Loss factor η
Configuration (a)				
Layer 1	0.49	1200	3.3×10^7	0.8
Layer 2	0.47	1250	3.3×10^8	0.6
Layer 3	0.45	1300	3.3×10^9	0.4
Layer 4	0.43	1350	3.3×10^{10}	0.2
Configuration (b)				
Layer 1	0.43	1350	3.3×10^{10}	0.2
Layer 2	0.45	1300	3.3×10^9	0.4
Layer 3	0.47	1250	3.3×10^8	0.6
Layer 4	0.49	1200	3.3×10^7	0.8

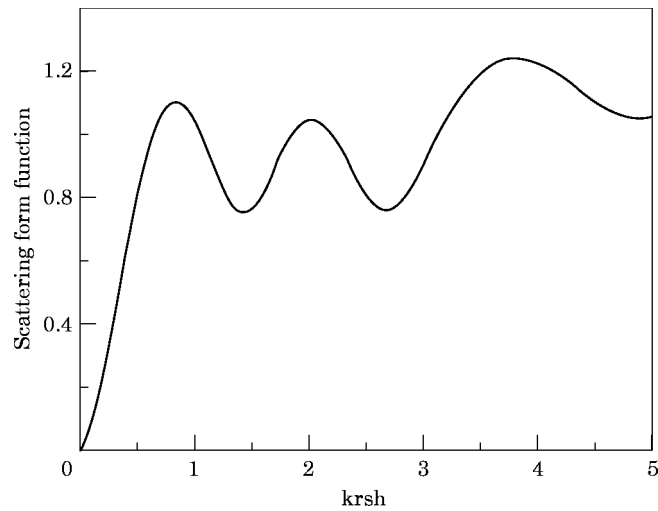


Figure 8. Scattering form function of a four-layer hose. —, Configuration (a); ----, configuration (b).

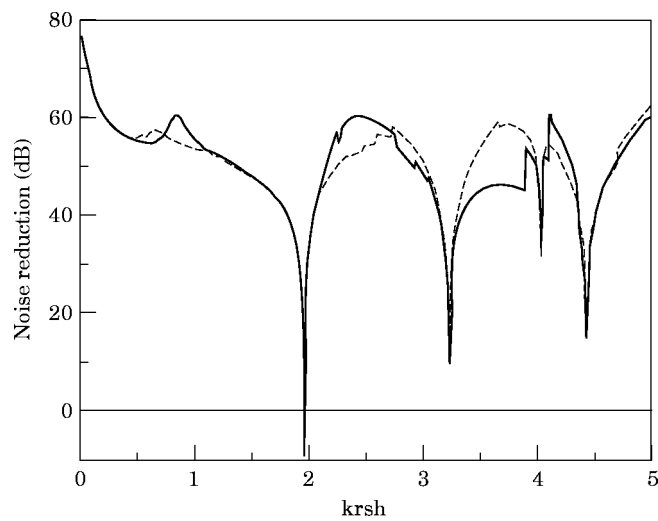


Figure 9. Noise reduction of a four-layer hose. —, Configuration (a); ----, configuration (b).

method may be applied readily to any number of layers, where the classical approach would be too cumbersome and susceptible to numerical instabilities.

7. CONCLUDING REMARKS

The transfer matrix presented here can be easily adapted to small or personal computers to evaluate the response of a multi-layer cylinder excited by a plane wave with two-dimensional pressure excitation. It has been shown to reduce to the 4×4 transfer matrix of reference [10] for the limiting case of normal or one-dimensional excitation. The overall transfer matrix elements can be obtained by multiplying the transfer matrices of successive layers by feeding in the elastic properties for the respective layers. Expressions are given for evaluation of the acoustic characteristics of the multi-layer cylinder. Numerical examples have been presented to illustrate the effect of two-dimensionality (angle of incidence) and the type of layer on scattering form function and noise reduction of a single layer, two-layer, and a four-layer cylinder.

ACKNOWLEDGMENTS

The authors would like to thank Dr. S. V. Raman, of NSTL and Mr. P. S. Kasthurirangan of GTRE, for the help and encouragement given to one of the authors (JSS) during the course of this work.

REFERENCES

1. L. FAX, V. K. VARADAN and V. V. VARADAN 1980 *Journal of the Acoustical Society of America* **68**, 1832–1835. Scattering of an obliquely incident acoustic wave by an infinite cylinder.
2. R. M. WHITE 1985 *Journal of the Acoustical Society of America* **30**, 771–785. Elastic wave scattering at a cylindrical discontinuity in a solid.
3. M. TALMANT, G. QUENTIN, J. L. ROUSSELOT, J. V. SUBRAHMANYAM and H. ÜBERALL 1988 *Journal of the Acoustical Society of America* **84**, 683–688. Acoustic resonances of thin cylindrical shells and the resonance scattering theory.
4. G. MAZE *et al.* 1990 *Journal of the Acoustical Society of America* **77**, 1352–1357. Resonances of plates and cylinders, and guided waves.
5. X.-L. BAO, H. CAO and H. ÜBERALL 1990 *Journal of the Acoustical Society of America*, **87**(1), 106–110. Resonances and surface waves in the scattering of an obliquely incident acoustic field by an infinite elastic cylinder.
6. F. LEON, F. LECROQ, D. DECULTOT and G. MAZE 1992 *Journal of the Acoustical Society of America* **91**, 1388–1397. Scattering of an obliquely incident acoustic wave by an infinite hollow cylindrical shell.
7. M. L. MUNJAL 1987 *Acoustics of Ducts and Mufflers*. New York: Wiley Interscience.
8. M. L. MUNJAL 1993 *Journal of Sound and Vibration* **162**, 333–344. Response of a multilayered infinite plate to an oblique plane wave by means of transfer matrices.
9. J. S. SASTRY and M. L. MUNJAL 1995 *Journal of Sound and Vibration* **182**, 109–128. A transfer matrix approach for evaluation of the response of a multi-layered infinite plate to a two-dimensional pressure excitation.
10. J. S. SASTRY and M. L. MUNJAL 1998 *Journal of Sound and Vibration*. **209**, 99–121. Response of a multi-layered infinite cylinder to a plane wave excitation by means of transfer matrices.
11. W. A. THOMSON 1950 *Journal of Applied Physics* **21**, 89–93. Transmission of elastic waves through a stratified solid medium.
12. L. M. BREKHOVISKIKH 1980 *Waves in Layered Media*. New York: Academic Press.
13. L. CREMER and M. HECKL 1988 *Structure Borne Sound*. Berlin: Springer Verlag; second edition.
14. M. ABRAMOWITZ and I. A. STEGUN 1964 *Handbook of Mathematical Functions*. Washington D.C.: National Bureau of Standards; first edition.

APPENDIX

The elements of the transfer matrix of equation (49) are as follows:

$$A_{1i} = -\frac{\pi G}{j\omega} \left[q_L r_{in} \left\{ \left(k_z^2 - \frac{k_T^2}{2} + \frac{n^2}{r_{out}^2} \right) \lambda_i - \frac{q_L}{r_{out}} \eta_i \right\} - \frac{q_T r_{in}}{r_{out}^2} \{ \eta \vartheta_i - n q_T r_{out} \xi_i + j k_z q_T r_{out}^2 \gamma_i \} \right],$$

$$A_{2i} = -\frac{\pi G}{j\omega} \left[\frac{q_L n r_{in}}{r_{out}^2} (\lambda_i - q_L r_{out} \eta_i) + \frac{q_T r_{in}}{r_{out}} \left\{ \left(\frac{q_T^2}{2} - \frac{n^2}{r_{out}^2} \right) r_{out} \vartheta_i \right. \right. \\ \left. \left. + q_T \xi_i - \frac{j k_z r_{out}}{2} q_T \gamma_i + \frac{j k_z}{2} (n+1) \chi_i \right\} \right],$$

$$A_{3i} = -\frac{\pi G}{2 j\omega} \left[-j k_z \left(2 q_L^2 r_{in} \eta_i + \frac{n q_T r_{in}}{r_{out}} \vartheta_i \right) + q_T r_{in} \left(k_T^2 - \frac{n^2}{r_{out}^2} - 2 k_z^2 + \frac{n+1}{r_{out}^2} \right) \chi_i - \frac{n q_T^2 r_{in}}{r_{out}} \gamma_i \right],$$

$$A_{4i} = -\frac{\pi}{2} \left[j k_z q_L r_{in} \lambda_i + q_T r_{in} \left\{ q_T \gamma_i + \frac{(n+1)}{r_{out}} \chi_i \right\} \right],$$

$$A_{5i} = -\frac{\pi}{2} \left[\frac{q_L n r_{in}}{r_{out}} \lambda_i + q_T r_{in} (q_T \xi_i + j k_z \chi_i) \right], \quad A_{6i} = \frac{\pi}{2} \left[q_L^2 r_{in} \eta_i + \frac{q_T r_{in}}{r_{out}} (n \vartheta_i - j k_z r_{out} \chi_i) \right].$$

Here the suffix $i = 1, 2, 3, 4, 5, 6$ used in the elements of matrix $[A]$ indicate the column. The variables $\lambda_i, \eta_i, \vartheta_i, \xi_i, \gamma_i, \chi_i, i = 1, 2, 3, 4, 5, 6$, are given by

$$\lambda_i = g_i P_{n,L} - f_i R_{n,L}, \quad \eta_i = g_i Q_{n,L} - f_i S_{n,L}, \quad \vartheta_i = l_i P_{n,T} - h_i R_{n,T}, \\ \xi_i = l_i Q_{n,T} - h_i S_{n,T}, \quad \gamma_i = t_i Q_{n+1,T} - p_i S_{n+1,T}, \quad \chi_i = t_i P_{n+1,T} - p_i R_{n+1,T},$$

where, in turn,

$$f_1 = j\omega/Gk_T^2, \quad f_2 = 0, \quad f_3 = 0, \quad f_4 = 2jk_z/k_T^2, \quad f_5 = 2n/k_T^2 r_{in}, \quad f_6 = 2/k_T^2 r_{in}, \\ h_1 = j\omega k_z^2/Gk_T^2 q_T^2, \quad h_2 = -j\omega/Gq_T^2, \quad h_3 = 0, \\ h_4 = (jk_z/q_T^2)(2k_z^2/k_T^2 - 1), \quad h_5 = (2/q_T^2 r_{in})(1 - nk_z^2/k_T^2), \quad h_6 = (2/q_T^2 r_{in})(n - k_z^2/k_T^2), \\ p_i = -(1/\Omega)\{jk_z n/r_{in}\}(h_i + f_i) + \Delta_p\}, \quad i = 1, 2, 3, 4, 5, 6, \quad \Omega = (2n+1)/r_{in}^2 + k_T^2, \\ \Delta_p = 0 \text{ for } i = 1, 2, 5, \quad \Delta_p = j\omega/G \text{ for } i = 3, \quad \Delta_p = n/r_{in} \text{ for } i = 4, \\ \Delta_p = -2jk_z \text{ for } i = 6, \\ t_i = -(1/q_T)\{jk_z f_i + [(n+1)/r_{in}]p_i + \Delta_t\}, \quad i = 1, 2, 3, 4, 5, 6, \\ \Delta_t = 0 \text{ for } i = 1, 2, 3, 4, 5, 6, \quad \Delta_t = 1 \text{ for } i = 4, \\ l_i = -(1/q_T)\{jk_z p_i + (n/r_{in})f_i + \Delta_l\}, \quad i = 1, 2, 3, 4, 5, 6, \\ \Delta_l = 0 \text{ for } i = 1, 2, 3, 4, 6, \quad \Delta_l = 1 \text{ for } i = 5,$$

$$g_i = (1/q_L) \{ j k_z p_i - (n/r_{in}) h_i + \Delta_g \}, \quad i = 1, 2, 3, 4, 5, 6,$$

$$\Delta_g = 0 \text{ for } i = 1, 2, 3, 4, 5, \quad \Delta_g = 1 \text{ for } i = 6,$$

$$P_{n,L} = J_n(q_L r_{in}) Y_n(q_L r_{out}) - Y_n(q_L r_{in}) J_n(q_L r_{out}),$$

$$Q_{n,L} = J_n(q_L r_{in}) Y'_n(q_L r_{out}) - Y_n(q_L r_{in}) J'_n(q_L r_{out}),$$

$$R_{n,L} = J'_n(q_L r_{in}) Y_n(q_L r_{out}) - Y'_n(q_L r_{in}) J_n(q_L r_{out}),$$

$$S_{n,L} = J'_n(q_L r_{in}) Y'_n(q_L r_{out}) - Y'_n(q_L r_{in}) J'_n(q_L r_{out}),$$

$$P_{n,T} = J_n(q_T r_{in}) Y_n(q_T r_{out}) - Y_n(q_T r_{in}) J_n(q_T r_{out}),$$

$$Q_{n,T} = J_n(q_T r_{in}) Y'_n(q_T r_{out}) - Y_n(q_T r_{in}) J'_n(q_T r_{out}),$$

$$R_{n,T} = J'_n(q_T r_{in}) Y_n(q_T r_{out}) - Y'_n(q_T r_{in}) J_n(q_T r_{out}),$$

$$S_{n,T} = J'_n(q_T r_{in}) Y'_n(q_T r_{out}) - Y'_n(q_T r_{in}) J'_n(q_T r_{out}),$$

$$P_{n+1,T} = J_{n+1}(q_T r_{in}) Y_{n+1}(q_T r_{out}) - Y_{n+1}(q_T r_{in}) J_{n+1}(q_T r_{out}),$$

$$Q_{n+1,T} = J_{n+1}(q_T r_{in}) Y'_{n+1}(q_T r_{out}) - Y_{n+1}(q_T r_{in}) J'_{n+1}(q_T r_{out}),$$

$$R_{n+1,T} = J'_{n+1}(q_T r_{in}) Y_{n+1}(q_T r_{out}) - Y'_{n+1}(q_T r_{in}) J_{n+1}(q_T r_{out}),$$

$$S_{n+1,T} = J'_{n+1}(q_T r_{in}) Y'_{n+1}(q_T r_{out}) - Y'_{n+1}(q_T r_{in}) J'_{n+1}(q_T r_{out}).$$